Biomedical Optics EXPRESS

Clinical evaluation of melanomas and common nevi by spectral imaging

Ilze Diebele,[1,*] Ilona Kuzmina,[1] Alexey Lihachev,[1] Janis Kapostinsh,[2] Alexander Derjabo,[2] Lauma Valeine,[3] and Janis Spigulis[1]

[1]*Biophotonics Laboratory, Institute of Atomic Physics and Spectroscopy, University of Latvia, Raina Blvd. 19, Riga, LV-1586, Latvia*
[2]*Latvian Oncology Center, Hipokrata Str. 4, Riga, LV-1006, Latvia*
[3]*Beauty Clinic "4th Dimension", Jeruzalemes Str. 1, Riga, LV-1010, Latvia*
**ilze.diebele@gmail.com*

Abstract: A clinical trial on multi-spectral imaging of malignant and non-malignant skin pathologies comprising 17 melanomas and 65 pigmented common nevi was performed. Optical density data of skin pathologies were obtained in the spectral range 450–950 nm using the multispectral camera Nuance EX. An image parameter and maps capable of distinguishing melanoma from pigmented nevi were proposed. The diagnostic criterion is based on skin optical density differences at three fixed wavelengths: 540nm, 650nm and 950nm. The sensitivity and specificity of this method were estimated to be 94% and 89%, respectively. The proposed methodology and potential clinical applications are discussed.

OCIS codes: (110.4234) Multispectral and hyperspectral imaging; (170.4580) Optical diagnostics for medicine.

References and Links

1. W. Klaus and J. R. Allen, *Fitzpatrick's Color Atlas & Synopsis of Clinical Dermatology* (McGraw-Hill Professional, New York, 2009).
2. B. D. Montgomery and G. M. Sadler, "Punch biopsy of pigmented lesions is potentially hazardous," Can. Fam. Physician **55**(1), 24 (2009).
3. B. Farina, C. Bartoli, A. Bono, A. Colombo, M. Lualdi, G. Tragni, R. Marchesini, B. Farina, C. Bartoli, A. Bono, A. Colombo, M. Lualdi, and G. Tragni, "Multispectral imaging approach in the diagnosis of cutaneous melanoma: potentiality and limits," Phys. Med. Biol. **45**(5), 1243–1254 (2000).
4. R. R. Anderson and J. A. Parrish, "The optics of human skin," J. Invest. Dermatol. **77**(1), 13–19 (1981).
5. G. Zonios, A. Dimou, I. Bassukas, D. Galaris, A. Tsolakidis, and E. Kaxiras, "Melanin absorption spectroscopy: new method for noninvasive skin investigation and melanoma detection," J. Biomed. Opt. **13**(1), 014017 (2008).
6. A. Garcia-Uribe, E. B. Smith, J. Zou, M. Duvic, V. Prieto, and L. V. Wang, "In-vivo characterization of optical properties of pigmented skin lesions including melanoma using oblique incidence diffuse reflectance spectrometry," J. Biomed. Opt. **16**(2), 020501 (2011).
7. I. Kuzmina, I. Diebele, D. Jakovels, J. Spigulis, L. Valeine, J. Kapostinsh, and A. Berzina, "Towards non-contact skin melanoma selection by multi-spectral imaging analysis," J. Biomed. Opt. **16**(6), 060502 (2011).
8. *User's Manual for Nuance 2.4.* (Cambridge Research & Instrumentation, Woburn, 2007).
9. Image processing and analysis in Java, ImageJ, *http://imagej.nih.gov/ij/*.
10. P. Thevenaz, "An ImageJ plugin for the automatic alignment of a source image or a stack to a target image," *http://bigwww.epfl.ch/thevenaz/turboreg/*.
11. S. Prahl, "Tabulated molar extinction coefficient for hemoglobin in water," *http://omlc.ogi.edu/spectra/hemoglobin/summary.html*.
12. T. Sarna and H. M. Swartz, "The physical properties of melanin," *http://omlc.ogi.edu/spectra/melanin/eumelanin.html*.

1. Introduction

Cutaneous melanoma currently represents 5% of newly diagnosed cancers in men and 6% in women; it is the leading fatal illness affecting the skin and is responsible for 80% of deaths from skin cancer [1]. It is hard to distinguish visually melanomas from non-malignant nevi. By now biopsy sampling from melanoma (which may increase the risk of spreading

#158653 - $15.00 USD Received 23 Nov 2011; revised 18 Jan 2012; accepted 18 Jan 2012; published 9 Feb 2012

metastases [2]) is the main method for making a precise diagnosis of the malformation. More patient-friendly non-invasive primary diagnostics would be preferable.

Multispectral imaging (MSI) is a non-contact, optical method that can be used in vivo with potentially promising applications to skin studies and pathology diagnosis [3]. Using narrow-band filtering at different wavelengths, a set of spectral images of the skin/pathology is taken; spectral filtering is usually performed by Liquid Crystal Tunable Filters or a set of discrete band pass filters. Each pixel of the image contains information about the corresponding skin spot at a specific wavelength, and a diffuse reflection spectrum for a single pixel can be obtained by processing the set of multi-spectral images. The penetration depth of optical radiation in the skin tissues depends on wavelength [4], so diffuse reflectance from skin at broadband illumination may provide morphological information from different depths, and multispectral imaging analysis makes it possible to extract this information [3,4].

The optical properties of melanin and of the different stages in a potentially malignant histological transition (dysplastic nevi → melanoma in situ → melanoma) have been investigated by contact diffuse reflectance [5]. Optical properties of benign and malignant pigmented lesions have also been measured by oblique incidence diffuse reflectance spectrometry [6]. Multispectral imaging provides spectral information over the entire area of the lesion and has potential for in vivo skin diagnostics, including melanoma diagnostics [7]. Previous investigations indicate that reflectance of the benign nevus at 940 nm is close to that of the surrounding skin, whereas pigmentation of the melanoma is detectable [3]. Consequently, combined visible and near infrared image analysis might help to distinguish melanomas from other skin malformations. In this study multispectral images were taken in the spectral range 450–950 nm in order to find a suitable algorithm that could be used for melanoma-nevus differentiation.

2. Methods and equipment

2.1 Experimental setup and processing algorithm

The measurement setup is shown in Fig. 1. The skin area to be studied is illuminated by a ring of halogen lamps. The light from the halogen lamps passes through a diffuser and a polarizing film. Reflected and back-scattered light from the skin passes through an objective lens into a multispectral imaging camera (Nuance EX). The Nuance Imaging Module contained the principal imaging components in a single compact enclosure: a high-resolution, scientific-grade CCD imaging sensor, a solid-state liquid crystal filter with a polarizer, a wavelength tuning element, a spectrally optimized lens and internal optics [8]. To avoid artifacts caused by light reflection from the skin surface, the polarization of the illuminating light was orthogonal to the orientation of polarizer located in the Nuance EX camera. Besides, the

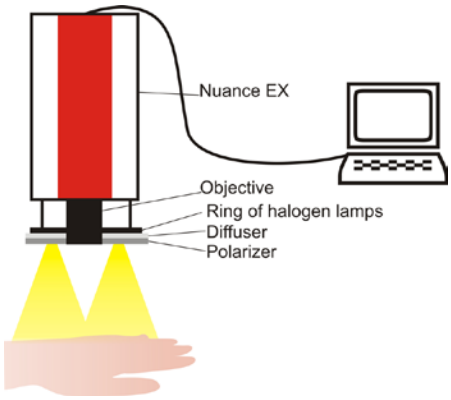

Fig. 1. The measurement setup: multispectral camera Nuance EX, halogen light source, polarizer, and computer.

#158653 - $15.00 USD Received 23 Nov 2011; revised 18 Jan 2012; accepted 18 Jan 2012; published 9 Feb 2012

halogen lamps were powered from a stabilized direct current source to avoid artifacts due to temporal fluctuations of the illumination. The Nuance program CRi was used to acquire image cubes and to average the spectra obtained from pigmented and normal skin areas.

During a clinical trial 82 pigmented lesions were studied by multispectral imaging in the wavelength range 450–950 nm. Spectra were obtained at different wavelengths over this range in steps of 10 nm. The half-bandwidth of the color filter that regulated each step was 15 nm. Overall, 17 histologically confirmed melanomas and 65 nevi identified by dermatologists were investigated in this study. The melanoma had different thickness: 8 melanomas fell in the thickness range from 1 to 2 mm and 9 within the thickness range of 3-5 mm (Breslow's depth). The nevi had diameters of at least 5 mm. 51 images at different wavelength bands were taken from each pigmented malformation. Before the measurement, the lesion was covered by white paper and a multispectral image set was taken, in order to record the illumination spectrum. Since white paper is not an ideal diffuse reflector, the spectral reflectance value was corrected by comparing it with an Avantes WS-2 reference tile (99%).. The respective corrections were further added to the captured image array using the same reference units (r.u.) that were also used for processing the pathology images.

All the measurements were taken from patients in supine position, in order to minimize the motion artifacts; in addition, the image stabilization program ImageJ [9] with plugin TurboReg [10] was used. During the image acquisition process the patients were asked to hold their breath about 30 seconds while the image cube was taken. The duration of the whole procedure depended on the location of malformation. The following steps of the procedure were taken:

- Patient relaxing in a comfortable recumbent position (about 1–3 minutes);
- Acquisition of the reference and image cube (about 1–2 minutes);
- Stabilization of the image cube, if necessary (about 5 minutes);
- Image processing (about 15 seconds).

The entire diagnostic process took about 15–20 minutes.

The optical density was calculated by the CRi Nuance program as

$$OD(\lambda) = -\log(I(\lambda) / I_0(\lambda)), \tag{1}$$

where I(λ) represents the intensity of the skin-reflected light and $I_0(\lambda)$, the intensity of the light reflected from the white etalon (at the same distance); λ denotes the wavelength.

In order to differentiate between melanoma and nevus, the following differentiation parameter *p* was proposed:

$$p = OD_{650} + OD_{950} - OD_{540} = \log\left(k \cdot \frac{I(540)}{I(650) \cdot I(950)} \right), \tag{2}$$

where

$$k = \frac{I_0(650) \cdot I_0(950)}{I_0(540)} \tag{3}$$

is the coefficient that describes the reference, and OD_{540}, OD_{650} and OD_{950} are the optical densities at 540nm, 650nm and 950 nm, respectively. The wavelength 540 nm corresponds to the wavelength of maximum absorption of the blood hemoglobin [11], while at 650 nm hemoglobin absorption is minimal and melanin absorption is more pronounced [12], and 950 nm is the wavelength at which light penetrates the skin surface most deeply [3] in our measurement conditions. The parameter *p* was calculated for each pixel, and then parametric *p*-images were constructed.

#158653 - $15.00 USD Received 23 Nov 2011; revised 18 Jan 2012; accepted 18 Jan 2012; published 9 Feb 2012

Figure 2 presents the patient-averaged spectra of the optical density for healthy skin (dark filled circles), common nevi (filled circles) and all melanomas (empty circles). Error bars representing one standard deviation are presented at few points of the curves to illustrate the statistical variation between patients. Each point of the mean OD spectra was calculated as the average value of all pixels in manually selected rectangular areas of regions of interest within and outside the lesions. For each lesion, the largest square area that could be completely enclosed in the lesion was selected, and an equivalent area of healthy skin outside the lesion was selected for comparison within the same image frame. The mean values of the *p*-parameters in Fig. 4 below were calculated in a similar way, by selecting a square area within each pathology that coincided with the region of higher *p*- parameter values.

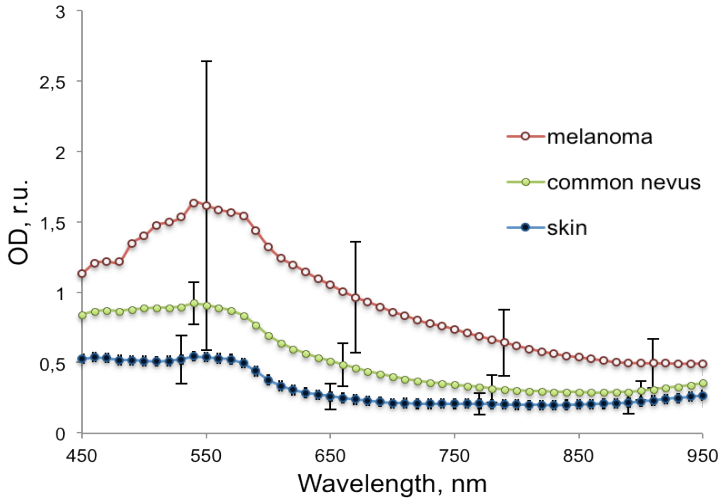

Fig. 2. The mean optical density spectra of 17 examined melanomas (empty circles), 65 common nevi (filled circles) and 82 healthy skin cases (dark filled circles).

3. Results and discussion

To illustrate the proposed differentiation parameter, Fig. 3 shows ordinary color RGB and parametric images of a melanoma and a nevus (a) and a pigmented nevus alone (b). The

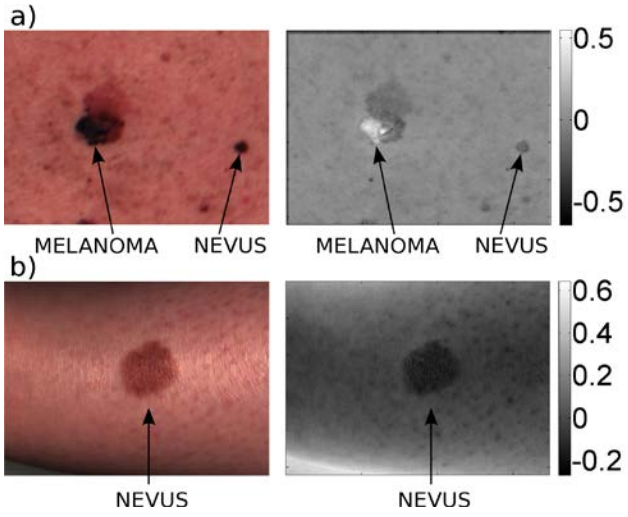

Fig. 3. RGB images (left) and parametric *p*-images (right) of melanoma (a) and pigmented nevus (b). The *p*-value of healthy skin is set to 0.

#158653 - $15.00 USD Received 23 Nov 2011; revised 18 Jan 2012; accepted 18 Jan 2012; published 9 Feb 2012

average *p*-value of healthy skin in these images is set to 0, in order to make the results comparable regardless of the individual skin type or color. The nevi regions in both cases are darker, while the melanoma region is lighter than the healthy skin background.

Most of the parametric *p*-maps of the examined lesions showed the same tendency—melanoma's areas (or parts of them) showed notably higher *p*-values than the surrounding skin, and the nevus areas showed lower *p*-values than the healthy skin, or, in some cases, similar *p*-values. Consequently, the criterion $p > p_0$, where p_0 is related to the surrounding healthy skin, may be regarded as indication to melanoma.

Figure 4 shows the scatter plot of the mean *p*-values (averaged over the selected pathology areas) for all examined cases of melanoma and common nevus, when p_0 is set to 0.

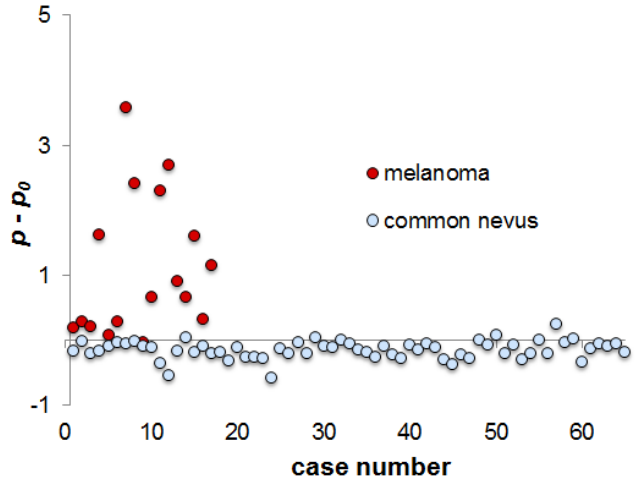

Fig. 4. Scatter plot of the normed p- parameter for all melanomas (dark circles) and nevi (light circles).

As the result of our diagnostic test, sensitivity, specificity, positive predictive value and negative predictive value were calculated. After analysis of the 17 available melanoma multi-spectral image sets, 16 showed clear response accordingly to the above-mentioned criterion *p* (true positives or TP), and only one case - melanoma with ulceration - did not support the criterion (false negative or FN). After analysis of 65 nevi, 58 of them showed lower *p*-parameter values than the surrounding skin, (true negatives or TN), and 7 cases did not meet the criterion (false positive or FP). Sensitivity of this test is TP/(TP + FN) = 94%, specificity is TN/(FP + TN) = 89%, positive predictive value (PPV) = TP/(TP + FP) = 70% and negative predictive value (NPV) = TN/(FN + TN) = 98%.

4. Conclusions

The reported results show that sensitivity and specificity of the proposed approach are high (94% and 89%, respectively). However, for clinical implementation it is necessary to verify this algorithm on a group of dysplastic nevi (the risk group of melanoma). But, presumably, there is a potential for clinical implementation, e.g. as additional test in cases when ABCD rule describing the four criteria of melanoma is not easy to apply, or in situations that cast doubts. Further studies would promote better understanding of the photophysiological processes in human skin and its lesions.

The image processing technique can be further improved. For instance, a simpler form of Eq. (2) can be used:

$$p' = k \cdot \frac{I(540)}{I(650) \cdot I(950)}, \tag{4}$$

#158653 - $15.00 USD Received 23 Nov 2011; revised 18 Jan 2012; accepted 18 Jan 2012; published 9 Feb 2012

where $k = \frac{I_0(650) \cdot I_0(950)}{I_0(540)}$. Besides, healthy skin also can be taken as a reference, and then $I_0(540)$, $I_0(650)$ and $I_0(950)$ will be reflection intensities from normal skin.

Improved software could replace the visual assessment (Figs. 2, 3) by automated selection of skin lesions in the future.

Acknowledgments

This work was supported by the European Social Fund, projects 2009/0138/1DP/1.1.2.1.2/09/IPIA/VIAA/004, 2009/0211/1DP/1.1.1.2.0/09/APIA/VIAA/077.

#158653 - $15.00 USD Received 23 Nov 2011; revised 18 Jan 2012; accepted 18 Jan 2012; published 9 Feb 2012